JOURNAL OF MATERIALS SCIENCE 20 (1985) 3125 – 3130

Defect structure and electrical conductivity in rapidly-quenched and slowly-cooled rhombohedral solid solutions of the system Bi_2O_3–BaO

TAKEYUKI SUZUKI, YOSHITAKA DANSUI, TETSUJI SHIRAI, CHIKAKO TSUBAKI
Department of Industrial Chemistry, Tokyo University of Agriculture and Technology, Koganeishi, Tokyo 184, Japan

The solid solubility limit, grain orientation, defect structure and electrical conductivity of solidified rhombohedral specimens in the Bi_2O_3–BaO system are described. The *c*-axes (in hexagonal notation) of solidified specimens were almost entirely oriented along the platelet/film thickness. Slow-cooling ($\sim 10^{-2}$ °C sec^{-1}) of the system gave solid solutions with substitutional type of $2BaO \rightarrow 2Ba'_{Bi} + 2O_O^{\times} + V_O^{\cdot\cdot}$ for 12 to 32 mol% BaO. High-temperature modification of slowly-cooled sample (16 mol% BaO) showed a conductivity of $8.8 \times 10^{-1}\,\Omega^{-1}\,cm^{-1}$ at 600° C along the conduction plane (perpendicular to the *c*-axis). Rapid quenching ($\sim 10^{5}$ °C sec^{-1}) produced solid solutions for 8 to 20 mol% BaO introducing interstitial Ba^{2+} (10–12 mol% BaO) and Schottky type defects such as V''''_{Bi} and $V_O^{\cdot\cdot}$ (16 to 20 mol% BaO), however the high-temperature modification of the rhombohedral structure could not be frozen.

1. Introduction

The search for oxide ion conductors suitable for low-temperature use ($< \sim 700$° C) has led solid electrolytes researchers to Bi_2O_3-based solid solutions. Although most solid solutions are concerned with the face centred cubic structure [1–4], a limited attempt has shown that the rhombohedral structure can also be a candidate for oxide ion conductors. Takahashi *et al.* [5, 6] found that sintered oxides of the Bi_2O_3–MO system (M = Ca, Sr, Ba) in the form of rhombohedral solid solutions have conductivities several times greater than those of stabilized zirconias. They also noticed an abrupt change of conductivity. Boivin and co-workers [7–11] prepared samples by fusion and slow-cooling and showed that the conduction was two dimensional; the conduction plane being perpendicular to *c*-axis (in hexagonal notation). The jump of conductivity was attributed to the $\beta_2 \rightarrow \beta_1$ transition within the rhombohedral structure. These features lead to attractive properties for many solid electrolyte applications. Among the earth–alkaline oxide dopants, BaO was chosen since the Bi_2O_3–BaO system has been partially studied by a solidification method, it has the lowest transition temperature, and the conductivity of the high-temperature modification, β_1, is $\sim 10^{-1}\,\Omega^{-1}\,cm^{-1}$ at around 600° C: one of the highest among the Bi_2O_3-based oxides. Our investigations were focused on the following aspects:

(1) quenching the high-temperature modification;

(2) the effect of solidification rate on the solubility limit and grain orientation;

(3) the compositional dependence of defect structure and electrical conductivity.

0022–2461/85 $03.00 + .12

2. Experimental details

The starting materials were Bi_2O_3 and $BaCO_3$ powders with 99.9% purity. Because of the paucity of phase diagram, it was necessary to conduct preliminary studies to determine liquidus temperatures. These were conducted by differential thermal analysis (DTA) in air at a heating rate of $10^\circ C\,min^{-1}$. The temperatures obtained were fitted with a smooth curve as a function of composition, in order to estimate the liquidus for 16 to 40 mol % BaO. For lower dopant levels, the liquidus by Levin and Roth [12] is available.

A mixture of the Bi_2O_3 and $BaCO_3$ powders was calcined in air for 1 h at about its liquidus to decompose the $BaCO_3$. The pre-fired specimens were powdered and used for solidification. The temperature of the melt in a platinum crucible was set initially to 150° C above the liquidus and then it was solidified by two methods: rapid-quenching and slow-cooling. Rapid-quenching was carried out by the single-roller method. This consists of spreading a melt on a rotating copper disk 20 cm in diameter, revolving at 2000 rpm. The quenching rate is estimated as $\sim 10^5\,^\circ C\,sec^{-1}$. Details of this technique have been given elsewhere [2, 3]. Slow-cooling of $\sim 10^{-2}\,^\circ C\,sec^{-1}$ was achieved by a conventional furnace-cool. Compositional variation of the samples were examined by reweighing the specimens after heat treatment. Solidified samples were investigated by X-ray diffractometry (using a Rigaku Denki SG-9) at room temperature. Cu$K\alpha$ radiation was used with a nickel filter. Grain orientation was deduced from the X-ray diffraction intensities of as-solidified specimens against those of finely ground powders using Lotgering's method [13]. Diffraction intensity was approximated by the peak height. The lattice parameters were obtained at a scanning speed of $0.25^\circ\,min^{-1}$ using silicon as the internal standard. Densities were determined by a standard pycnometric method using n-butanol at room temperature. Reduced atmospheric pressure generated by a rotary pump facilitated extraction of gaseous inclusion at the liquid–sample interface. Total electrical conductivity was measured in the heating-up direction by means of the complex impedance method [14] over the frequency range 1 Hz to 100 kHz by use of phase-sensitive detector (NF circuit design block: LI-575). Painted silver paste was used as electrodes. All measurements was performed in air.

3. Results and discussion

DTA measurements gave the liquidus as 750, 730, 733, 760, 773, 803 and 823°C at 16, 20, 22, 28, 30, 36 and 40 mol % BaO, respectively. During melting of the Bi_2O_3–BaO, vaporization was observed, however it was low. Reweighing the samples after heat treatment at 800° C, followed by slow-cooling, showed losses less than 0.15%. These losses were neglected and we assumed that the nominal compositions and valencies (Bi^{3+} and Ba^{2+}) were kept throughout the experiments. No sticking of the samples to the Pt cruicible was observed. Rapidly-quenched specimens were film-shaped, typically 2 cm long, 0.5 to 1 mm wide and 15 μm thick. The slowly-cooled ingot was easily cleaved into yellowish mica-like platelets by a knife edge when it formed the rhombohedral solid solution. The thickness varied from 20 to 70 μm.

3.1. Solidified phase

Shown in Table I is the monophasic rhombohedral solid solution range and the unit cell volume. These ranges may be compared to the previously reported rhombohedral phase diagram of Boivin *et al.* [11], where the stable rhombohedral composition extends from 26 to 30 mol % BaO at 500° C. Rapid-quenching

TABLE I Monophasic rhombohedral solid solution range and the unit cell volume

Quenched film		Slowly cooled platelet	
mol % BaO	Unit cell volume (nm^3)	mol % BaO	Unit cell volume (nm^3)
8	0.1297 ± 0.0003	12	0.1299 ± 0.0002
10	0.1300 ± 0.0006	16	0.1307 ± 0.0002
12	0.1305 ± 0.0002	20	0.1315 ± 0.0005
14	0.1302 ± 0.0002	24	0.1314 ± 0.0007
16	0.13095 ± 0.0003	28	0.1329 ± 0.0002
18	0.1307 ± 0.0002	32	0.1341 ± 0.0003
20	0.1313 ± 0.0002		

produced the rhombohedral structure between 8 to 20 mol % BaO and mixtures of rhombohedral and body centered cubic structure from 22 to 38 mol % BaO. When mixtures were formed the colour changed gradually from yellow to purplish red. A large extension of solid solubility limit was achieved towards the lower BaO content. Slow-cooling resulted in a rhombohedral solid solution between 12 to 32 mol % BaO.

Boivin *et al.* [7, 11] reported that the *c*-parameter increased suddenly when the high-temperature modification was formed, but that the high-temperature form could not be retained by their slow-cooling ($\sim 10^{-3}\,^{\circ}\mathrm{C\,sec^{-1}}$). In order to see if the high-temperature form was frozen in the present experiments, we calculated the C-parameter. Slowly-cooled specimens gave 2.850(1), 2.858(3) and 2.855(2) nm at 12, 16 and 20 mol % BaO, respectively. Corresponding parameters of the rapidly-quenched specimens were 2.853(3), 2.852(6) and 2.855(2) nm. A comparison of these values shows, indirect as it is, that even the rapid-quenching could not retain the high-temperature modification. A more direct evidence, conductivity jump, is discussed in Section 3.3.

Orientation degree is defined so that it is 100 % when the *c*-axis lies parallel along the sample thickness and 0% for perfect randomness. The *c*-axis of solidified specimens were oriented, almost entirely, along the platelet/film thickness as shown in Table II. Relatively low grain orientation was observed at the solubility limits of the quenched films. Since the conduction plane is perpendicular to the *c*-axis (specimen thickness), a suitable solid electrolyte design may be required to take advantage of the conduction anisotropy.

3.2. Defect structure

When BaO is added to Bi_2O_3, a general solid solution formation reaction can be expressed using Kröger–Vink notation [15], as

$$\mathrm{BaO} \rightarrow a\mathrm{Ba}'_{\mathrm{Bi}} + b\mathrm{Ba}_{\mathrm{i}}^{\cdot\cdot} + c\mathrm{V}'''_{\mathrm{Bi}} + d\mathrm{O}''_{\square} + e\mathrm{O}_0^{\mathrm{x}} + f\mathrm{V}_0^{\cdot\cdot}$$

Mass and charge balance require the following relationships;

$$1 = a + b,\ 1 = d + e,$$

$$a + 3c + 2d = 2b + 2f$$

The original rhombohedral cell may be expressed as $Bi_3O_{4.5}\square_{1.5}$ after Sillen and Aurivillius [16]. Taking account of the cationic lattice point number 3, the unit cell formula of the composition $(Bi_2O_3)_{1-x}(BaO)_x$ is given by,

$$\mathrm{Bi}_{2g(1-x)}\mathrm{Ba}_{gx}\mathrm{O}_{g(3-2x)}\square_{g[1-(1-d)x]}$$

where x is the mole fraction and $g = 3/[2 - (2 - a - c)x]$. Five sample reaction models and the resultant unit cell formulas are given in Table III. Fig. 1 compares measured and calculated densities of slowly-cooled specimens. Calculated densities are traced by two straight lines joining at 24 mol % BaO, while measured values are plotted in the 90% reliability interval.

The formation reaction of solid solution follows Model 4. In Fig. 2 the densities of rapidly-quenched specimens combined with those of slowly-cooled specimens are given. The measured density of the lower solubility limit (8 mol % BaO) is not plotted because of the poor reproducibility. Calculated values were approximated by 4 straight lines: 8–12, 12–14 and 14–20 mol % BaO using rapidly-quenched unit cell volumes and 24–32 mol % BaO using unit cell volumes of slowly-cooled samples. Specimens having 10 and 12 mol % BaO follow Model 2, while those of 16, 18 and 20 mol % BaO are situated between Models 4 and 5. Rapidly-quenched specimens are characterized by the occurrence of interstitial Ba^{2+} at low

TABLE II Grain orientation of *c*-axis along the platelet/film thickness

Quenched film		Slowly cooled platelet	
mol % BaO	Orientation (%)	mol % BaO	Orientation (%)
8	73	12	98
10	98	16	100
12	98	20	100
14	98	24	100
16	93	28	100
18	92	32	100
20	88		

TABLE III Typical reaction model and the unit cell formula

	Reaction	Unit cell formula			
1	$BaO \rightarrow Ba^{\cdot\cdot}i + O''_{\square}$	Bi 3	Ba $\frac{3x}{2(1-x)}$	O $\frac{3(3-2x)}{2(1-x)}$	□ $\frac{3(1-2x)}{2(1-x)}$
2	$6BaO \rightarrow 2Ba'_{Bi} + 4Ba^{\cdot\cdot}i + 3O''_{\square} + 3O^{x}_{0}$	Bi $\frac{18(1-x)}{6-5x}$	Ba $\frac{9x}{6-5x}$	O $\frac{9(3-2x)}{6-5x}$	□ $\frac{9(2-3x)}{2(6-5x)}$
3	$3BaO \rightarrow 2Ba'_{Bi} + Ba^{\cdot\cdot}i + 3O^{x}_{0}$	Bi $\frac{9(1-x)}{3-2x}$	Ba $\frac{9x}{2(3-2x)}$	O 4.5	□ $\frac{9(1-x)}{2(3-2x)}$
4	$2BaO \rightarrow 2Ba'_{Bi} + 2O^{x}_{0} + V^{\cdot\cdot}_{0}$	Bi $\frac{6(1-x)}{2-x}$	Ba $\frac{3x}{2-x}$	O $\frac{3(3-2x)}{2-x}$	□ $\frac{3(1-x)}{2-x}$
5	$3BaO \rightarrow 3Ba'_{Bi} + V'''_{Bi} + 3O^{x}_{0} + 3V^{\cdot\cdot}_{0}$	Bi $\frac{9(1-x)}{3-x}$	Ba $\frac{9x}{2(3-x)}$	O $\frac{9(3-2x)}{2(3-x)}$	□ $\frac{9(1-x)}{2(3-x)}$

dopant level (10 to 12 mol% BaO) and the formation of Schottky type defects such as V'''_{Bi} and $V^{\cdot\cdot}_{0}$ at high dopant level (16 to 20 mol% BaO). Formation of substitutional solid solution (Model 4) is also observed in the Bi_2O_3–CaO system, however neither interstitial cations nor Schottky type defects are formed by quenching in liquid nitrogen [7].

3.3. Electrical conductivity

Fig. 3 shows the isothermal conductivity along the platelet/film plane plotted against BaO content. A typical example of Arrhenius plots of 16 mol% BaO is represented in Fig. 4. (No plot of slowly-cooled sample is given at 550° C as it changed greatly during impedance measurement.) It is clear that the high-temperature modification was not quenched because compositions having 16 to 28 mol% BaO exhibited a conduction jump between 500 to 600° C. The conductivities of slowly-cooled specimens were 8.8×10^{-1}, 7.3×10^{-1}, 5.3×10^{-1} and 4.6×10^{-1} $(\Omega cm)^{-1}$ at 16, 20, 24 and 28 mol% BaO, respectively. No sample destruction accompanied this structural modification. For 12 mol% BaO, the quenched sample showed a phase change from rhombohedral to another structure (not examined) above 500° C and the slowly-cooled sample had a continuous change of conductivity. The lower conductivity of the quenched samples relative to the slowly-cooled samples may be attributed to the immoderately introduced interstitial Ba^{2+} between 300 to 400° C. Quenched monophasic rhombohedral

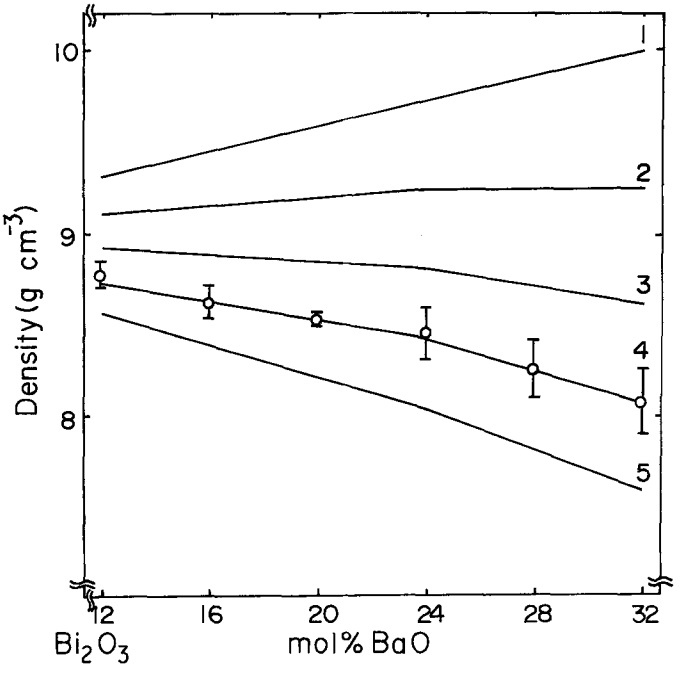

Figure 1 Comparison of measured and calculated desnity of slowly-cooled specimens.

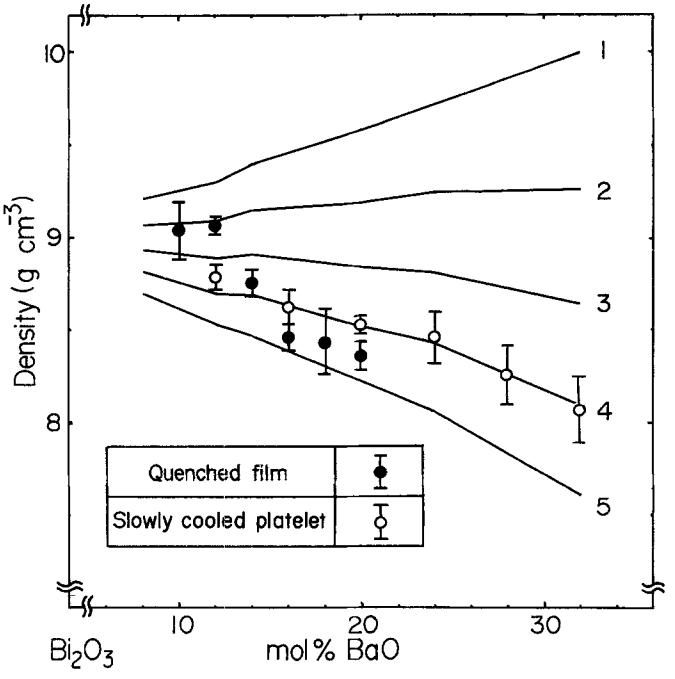

Figure 2 Comparison of measured and calculated density of rapidly-quenched and slowly cooled specimens.

solutions (12 to 20 mol % BaO) showed higher conductivities in the lower-temperature form and lower conductivities in the high-temperature form than the mixed phase specimens (24 to 28 mol % BaO). The ionic nature of the conductivity remains to be studied.

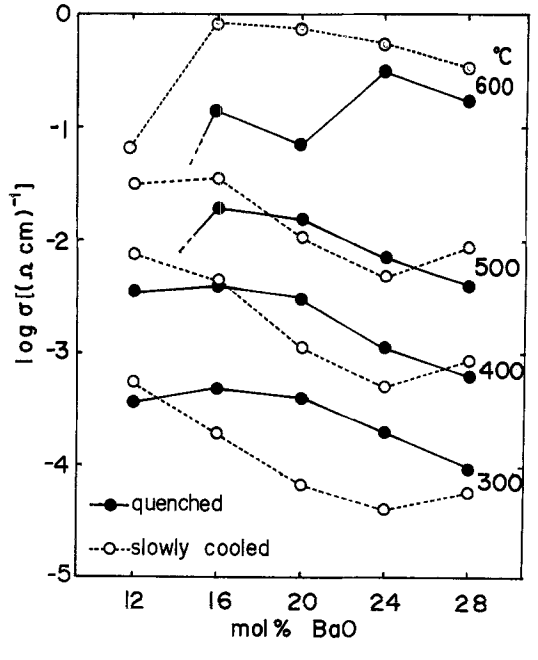

Figure 3 Isothermal conductivity plots along the platelet/film plane against BaO content.

4. Conclusions

(a) In the Bi_2O_3–BaO system, rhombohedral solid solutions were formed for 12 to 32 mol % BaO by slow-cooling ($\sim 10^{-2}$° C per sec) and for 8 to 20 mol % BaO by rapid-quenching ($\sim 10^{5}$° C^{-1}).

(b) Solid solution formation of the type $2BaO \rightarrow 2Ba'_{Bi} + 2O^{x}_{0} + V^{\cdot\cdot}_{0}$ occurred in slowly-cooled specimens (12 to 32 mol % BaO), while rapidly-quenched specimens showed formation of interstitial Ba^{2+} (10 to 12 mol % BaO) and Schottky type defects such as V'''_{Bi} and $V^{\cdot\cdot}_{0}$ (16 to 20 mol % BaO).

(c) The *c*-axes of solidified specimens were almost entirely oriented along the platelet/film thickness.

(d) The high-temperature modification of the rhombohedral structure could not be retained by rapid-quenching.

(e) The high-temperature modification of slowly-cooled specimen (16 mol % BaO) showed a conductivity of 8.8×10^{-1} $(\Omega\,cm)^{-1}$ at 600° C along the conduction plane (perpendicular to *c*-axis).

References

1. E. C. SUBBARAO and H. S. MAITI, *Solid State Ionics* **11** (1984) 317.
2. T. SUZUKI and S. UKAWA, *J. Mater. Sci.* **18** (1983) 1845.

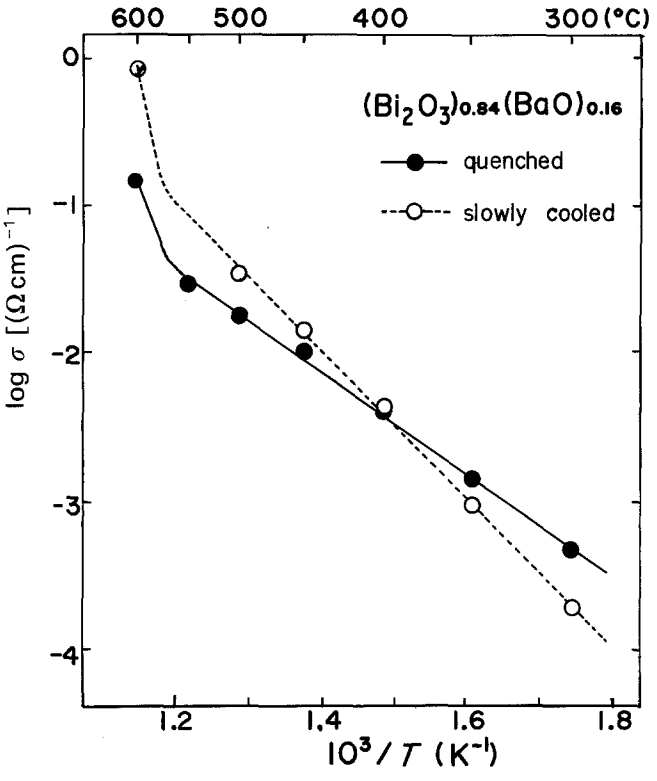

Figure 4 Conductivity against the reciprocal of absolute temperature for 16 mol % BaO.

3. T. SUZUKI, S. UKAWA, M. MORITA and K. HOSHI, Proceedings of the International Meeting on Chemical Sensors, Fukuoka, September 1983, edited by T. Seiyama, K. Fueki, J. Shiokawa and S. Suzuki (Kodansha/Elsevier, Tokyo, 1983) p. 256.
4. T. SUZUKI, K. KAKU, S. UKAWA and Y. DANSUI, *Solid State Ionics* **13** (1984) 237.
5. T. TAKAHASHI, H. IWAHARA and Y. NAGAI, *J. Appl. Electrochem.* **2** (1972) 97.
6. T.TAKAHASHI, T.ESAKA and H. IWAHARA, *J. Solid State Chem.* **16** (1976) 317.
7. P. CONFLANT, J. C. BOIVIN and D. THOMAS, *ibid.* **18** (1976) 133.
8. *Idem, ibid.* **35** (1980) 192.
9. J. C. BOIVIN and D. J. THOMAS, *Solid State Ionics* **3/4** (1981) 457.
10. *Idem, ibid.* **5** (1981) 523.
11. P. CONFLANT, J. C. BOIVIN, G. NOWOGROCKI and D. THOMAS, *ibid.* **9/10** (1983) 925.
12. E. M. LEVIN and R. S. ROTH, *J. Res. Nat. Bur. Stand.* **68A2** (1964) 202.
13. F. K. LOTRERING, *J. Inorg. Nucl. Chem.* **9** (1959) 113.
14. J. E. BAUERLE, *J. Phys. Chem. Solids* **30** (1967) 2657.
15. F. A. KRÖGER, "The Chemistry of Imperfect Crystals, Vol. II" (North-Holland, Amsterdam, 1974) p. 1.
16. L. G. SILLEN and B. AURIVILLIUS, *Z. Kristallogr.* **101** (1939) 483.

Received 5 September
and accepted 1 October 1984